

Thermodynamics, Transport, and Fluid Mechanics

## Experimental and CPA EoS Description of the Key Components in the BTX Separation from Gasolines by Extractive Distillation with Tricyanomethanide-based Ionic Liquids

Miguel Ayuso, André M. Palma, Marcos Larriba, Noemí Delgado Mellado, Julian Garcia,  
Francisco Rodríguez, Joao A.P. Coutinho, Pedro Jorge Carvalho, and Pablo Navarro

*Ind. Eng. Chem. Res.*, **Just Accepted Manuscript** • DOI: 10.1021/acs.iecr.0c02844 • Publication Date (Web): 24 Jul 2020

Downloaded from [pubs.acs.org](https://pubs.acs.org) on July 27, 2020

### Just Accepted

“Just Accepted” manuscripts have been peer-reviewed and accepted for publication. They are posted online prior to technical editing, formatting for publication and author proofing. The American Chemical Society provides “Just Accepted” as a service to the research community to expedite the dissemination of scientific material as soon as possible after acceptance. “Just Accepted” manuscripts appear in full in PDF format accompanied by an HTML abstract. “Just Accepted” manuscripts have been fully peer reviewed, but should not be considered the official version of record. They are citable by the Digital Object Identifier (DOI®). “Just Accepted” is an optional service offered to authors. Therefore, the “Just Accepted” Web site may not include all articles that will be published in the journal. After a manuscript is technically edited and formatted, it will be removed from the “Just Accepted” Web site and published as an ASAP article. Note that technical editing may introduce minor changes to the manuscript text and/or graphics which could affect content, and all legal disclaimers and ethical guidelines that apply to the journal pertain. ACS cannot be held responsible for errors or consequences arising from the use of information contained in these “Just Accepted” manuscripts.

# Experimental and CPA EoS Description of the Key Components in the BTX Separation from Gasolines by Extractive Distillation with Tricyanomethanide-based Ionic Liquids

Miguel Ayuso<sup>a</sup>, André M. Palma<sup>b</sup>, Marcos Larriba<sup>a</sup>, Noemí Delgado-Mellado<sup>a</sup>, Julián García<sup>a</sup>, Francisco Rodríguez<sup>a</sup>, João A.P. Coutinho<sup>b</sup>, Pedro J. Carvalho<sup>b</sup>, Pablo Navarro<sup>b,c,\*</sup>

<sup>a</sup> Department of Chemical and Materials Engineering, Complutense University of Madrid, E-28040 Madrid, Spain.

<sup>b</sup> CICECO – Aveiro Institute of Materials, Department of Chemistry, University of Aveiro, Aveiro, Portugal.

<sup>c</sup> Department of Chemical Engineering, Autónoma University of Madrid, E-28049 Madrid, Spain.

## Abstract

Two tricyanomethanide-based ionic liquids (ILs), namely 1-ethyl-3-methylimidazolium tricyanomethanide ([C<sub>2</sub>C<sub>1</sub>im][TCM]) and 1-butyl-4-methylpyridinium tricyanomethanide ([4-C<sub>4</sub>C<sub>1</sub>py][TCM]) have been recently reported as effective solvents for the BTX extractive distillation from pyrolysis gasoline. The vapor-liquid or vapor-liquid-liquid equilibria (VLE/VLLE) of several {aliphatic + aromatic + [TCM]-based ILs} ternary systems related to pyrolysis gasoline was extensively determined by headspace-gas chromatography (HS-GC), on a wide range of temperatures and solvent-to-feed (S/F) ratios. The Cubic Plus Association Equation of State (CPA EoS) was used to predictively describe the experimental VLE/VLLE from binary interaction parameters regressed from {hydrocarbon + IL} binary systems. Here, the VLE/VLLE related to the separation of the pyrolysis gasoline key components (*n*-octane and benzene) and other aliphatic/aromatic challenging mixtures in terms of aliphatic/aromatic relative volatility is reported. Specifically, the VLE/VLLE data for {*n*-octane + benzene + IL}, {*n*-heptane + benzene + IL} and {*n*-octane + toluene + IL} ternary systems were determined. The CPA EoS accuracy, robustness, and transferability between different systems is verified, with the advantages and limitations shown in previous works. Overall, the results obtained in this work lay the foundation for the implementation of the CPA EoS parametrization in a commercial simulator to rigorously simulate the multicomponent BTX extractive distillation from pyrolysis gasoline with ILs.

**Keywords:** Ionic liquids; aromatic/aliphatic separation; extractive distillation; Headspace-Gas Chromatography; CPA EoS

\* To whom correspondence should be addressed. E-mail address: pablo.navarro@uam.es (Pablo Navarro).

## 1. Introduction

Extractive distillation is commonly used in the petrochemical industry to separate mixtures that cannot be addressed by conventional distillation due to the presence of close-boiling compounds and azeotropes.<sup>1,2</sup> In these cases, a mass separating agent is added as an additional feed stream to modify the activity coefficients, increasing the relative volatility of the key components in the mixture.<sup>3</sup> One of the main applications of the extractive distillation is the separation of aromatic hydrocarbons, mainly benzene, toluene, and xylenes (BTX), from refinery streams with high-aromatic content, such as pyrolysis gasoline (66.1 wt.%).<sup>1</sup> Current mass separating agents used in conventional BTX extractive distillation processes are organic compounds, namely sulfolane, *N*-methylpyrrolidone or *N*-formylmorpholine, among others. These mass separating agents present several drawbacks, such as their flammability, volatility and toxicity, leading to a negative environmental impact. The conventional BTX extractive distillation processes present high energy consumption and operating costs, owing to the losses and high boiling points of solvents.<sup>4</sup> Therefore, the selection of a suitable solvent is a crucial step to ensure an effective, economical and sustainable extractive distillation process.<sup>5–11</sup>

Lately, ionic liquids (ILs) have received great interest from researchers due to their remarkable characteristics that favor their use as mass separating agents: negligible vapor pressure, broad liquid range<sup>12</sup> and high thermal and chemical stability.<sup>13</sup> Also, ILs can be considered as designer solvents due to the possibility of tuning their extractive and physical properties through the combination of different anions and cations<sup>14</sup> or through carefully planning IL mixtures.<sup>15–18</sup> ILs have been successfully tested as mass agents in extractive distillation processes for the separation of different mixtures,<sup>8,19–26</sup> with special impact in those containing aromatic compounds.<sup>27–35</sup> The promising results have prompted the IL-based extractive distillation as a potential alternative to current extractive distillation processes, reducing energy consumption, and, at the same time, enhancing purity standards in only one piece of equipment.<sup>36–38</sup>

In previous works, tricyanomethanide-based ILs were selected as the most appropriate ILs for the aromatic/aliphatic extractive distillation.<sup>39</sup> This selection was based on the extensive liquid-liquid equilibria data reported to {alkane + aromatic + IL} ternary systems and their relatively low viscosity and high thermal stability.<sup>40</sup> Afterwards, the experimental characterization of the VLE/VLLE for several {aliphatic/aromatic + IL} binary systems and {aliphatic + aromatic + IL} ternary systems was made by headspace-gas chromatography (HS-GC) using the 1-ethyl-3-methylimidazolium tricyanomethanide ([C<sub>2</sub>C<sub>1</sub>im][TCM]) and 1-butyl-4-methylpyridinium

1  
2 65 tricyanomethanide ([4-C<sub>4</sub>C<sub>1</sub>py][TCM]) as mass agents.<sup>41</sup> The CPA EoS was used to model the  
3  
4 66 phase equilibria, and its accuracy and robustness were demonstrated in wide ranges of S/F ratios  
5  
6 67 and temperatures. The transferability of the CPA EoS binary interaction parameters between  
7  
8 68 different systems, and their dependence with molecular weight and temperature were also  
9  
10 69 checked.<sup>41,42</sup>

11 70 This work deepens in the study of the BTX separation from pyrolysis gasoline by extractive  
12  
13 71 distillation with tricyanomethanide-based ILs. Taking into account the composition of a  
14  
15 72 pyrolysis gasoline model available in the literature,<sup>1</sup> the light and heavy key components of this  
16  
17 73 gasoline model are *n*-octane and benzene, respectively. Thus, the *n*-octane/benzene separation  
18  
19 74 is the most challenging within the overall separation. Also, *n*-heptane/benzene and *n*-  
20  
21 75 octane/toluene are the other difficult separations in terms of aliphatic/aromatic relative  
22  
23 76 volatility. Taking advantage of the above mentioned background, the VLE/VLLE for {*n*-octane  
24  
25 77 + benzene + [C<sub>2</sub>C<sub>1</sub>im][TCM] or [4-C<sub>4</sub>C<sub>1</sub>py][TCM]}, {*n*-heptane + benzene + [C<sub>2</sub>C<sub>1</sub>im][TCM]  
26  
27 78 or [4-C<sub>4</sub>C<sub>1</sub>py][TCM]}, and {*n*-octane + toluene + [C<sub>2</sub>C<sub>1</sub>im][TCM] or [4-C<sub>4</sub>C<sub>1</sub>py][TCM]}  
28  
29 79 ternary systems were studied in the whole hydrocarbon composition range for a S/F ratio of 10  
30  
31 80 at the temperatures of 323.2, 363.2 and 403.2 K. The VLE/VLLE experimental data was also  
32  
33 81 used to validate the CPA EoS model obtained in previous works, confirming its robustness.<sup>41,42</sup>  
34  
35 82 Furthermore, the CPA EoS ability to describe dramatic changes in relative volatility in favor of  
36  
37 83 the aliphatics, the so-called flipping phenomenon,<sup>43</sup> is evaluated, creating the bases for the  
38  
39 84 CPA EoS parameters implementation in a commercial simulator like Aspen Plus.

## 36 85 **2. Experimental Section**

### 37 86 **2.1. Chemicals**

38  
39 87 The two ILs, namely 1-ethyl-3-methylimidazolium tricyanomethanide, [C<sub>2</sub>C<sub>1</sub>im][TCM], and 1-  
40  
41 88 butyl-4-methylpyridinium tricyanomethanide, [4-C<sub>4</sub>C<sub>1</sub>py][TCM], were supplied by Iolitec  
42  
43 89 GmbH with a mass purity of at least 98 %. The ILs were further purified at vacuum conditions  
44  
45 90 (50 Pa) and moderate temperature (313 K) before the measurements. The aliphatic and aromatic  
46  
47 91 hydrocarbons were purchased from Sigma-Aldrich with mass fraction purity greater than 99%.  
48  
49 92 The hydrocarbons were kept in their original vessels over 3 Å molecular sieves and were  
50  
51 93 handled inside a glove box to avoid water absorption from ambient humidity. Specifications of  
52  
53 94 the chemicals are reported in Table 1.

95 **Table 1. Chemicals: Suppliers, Purities and Water Contents**

Chemical	Supplier	Purity in wt. %	Water content in ppm
1-ethyl-3-methylimidazolium tricyanomethanide [C <sub>2</sub> C <sub>1</sub> im][TCM]	Iolitec GmbH	98.0	< 300
1-butyl-4-methylpyridinium tricyanomethanide [4-C <sub>4</sub> C <sub>1</sub> py][TCM]	Iolitec GmbH	98.0	< 300
<i>n</i> -heptane	Sigma-Aldrich	99.7	Anhydrous
<i>n</i> -octane	Sigma-Aldrich	≥ 99.0	Anhydrous
benzene	Sigma-Aldrich	99.8	Anhydrous
toluene	Sigma-Aldrich	99.5	Anhydrous

96 <sup>a</sup>Karl Fischer titration method97 **2.2. Determination of VLE/VLLE**

98 The isothermal VLE and VLLE data were experimentally obtained using an Agilent 7697A  
 99 headspace injector coupled to an Agilent 7890A gas chromatograph (HS-GC). This technique  
 100 was widely explained in previous work.<sup>44</sup> Firstly, feed mixtures were gravimetrically prepared  
 101 in 20 mL glass vials using a Mettler Toledo XS205 balance with a precision of 10<sup>-5</sup> g. After,  
 102 the mixtures were stirred inside the oven and allowed to reach the equilibrium, for time never  
 103 smaller than 2 h.

104 A sample of the vapor phase was taken by the HS and analyzed by GC to obtain its composition  
 105 ( $y_i$ ). Knowing the feed ( $z_i$ ) and the vapor phase composition ( $y_i$ ), the overall liquid phase  
 106 composition ( $x_i$ ) can be determined by mass balance as follows:

$$107 \quad x_i = \frac{z_i \cdot F - (p_i \cdot V_G / R \cdot T)}{\sum_{i=1}^3 (z_i \cdot F - (p_i \cdot V_G / R \cdot T))} \quad (1)$$

108 where  $F$  denotes the molar amount of the feed,  $V_G$  is the headspace volume of the vial,  $R$  is the  
 109 ideal gas law constant,  $N$  is the number of components and  $p_i$  is the partial pressure of the  
 110 component  $i$  calculated as follows:

$$111 \quad p_i = \frac{p_i^0 \cdot A_i}{A_i^0} \quad (2)$$

112 where  $A_i$  is the peak areas of the hydrocarbons,  $A_i^0$  the peak areas of each pure hydrocarbon at  
 113 the same conditions and  $p_i^0$  the vapor pressure of each pure component from the literature.<sup>45</sup>

1  
2 114 As explained in previous work,<sup>39</sup> for those assays presenting liquid-liquid phase splitting, an  
3  
4 115 additional vial was prepared to determine the composition of one of the liquid phases. A sample  
5  
6 116 of the IL-rich liquid phase was directly taken with a syringe and analyzed by multiple headspace  
7  
8 117 extraction (MHE). Hence, knowing the composition of the vapor phase ( $y_i$ ) and the IL-rich  
9  
10 118 liquid phase ( $x_{IL,i}$ ), the amount of the liquid phases ( $L_{II}$  and  $L_I$ ) and the composition of IL-free  
11  
12 119 liquid phase ( $x_{I,i}$ ) were determined by mass balance as detailed elsewhere<sup>39</sup>.

### 120 3. CPA EoS Model

121 Kontogeorgis et al.<sup>46,47</sup> proposed a simplified CPA EoS version with two terms: a physical  
122 contribution term from the Soave Redlich-Kwong (SRK) EoS and an association term that takes  
123 into account the specific site-site intermolecular interaction. The CPA EoS approach is  
124 expressed in terms of the compressibility factor ( $Z$ ) as the sum of physical and association  
125 contributions:

$$126 \quad Z = Z^{\text{phys}} + Z^{\text{assoc}} \quad (3)$$

127 In this work, the parameters from physical ( $a$ ,  $b$  and  $c_0$ ) and association ( $\beta$  and  $\epsilon$ ) terms for the  
128 hydrocarbons (non-associative compounds) and the tricyanomethanide-based IL (associative  
129 compounds) were taken from previous works,<sup>41,42</sup> where the IL non-volatile character was  
130 carefully described. The parameters  $a$  and  $b$  are calculated following the well-known vdW-1f  
131 mixing rules:

$$132 \quad a = \sum_i \sum_j x_i x_j a_{ij} \quad ; \quad a_{ij} = a_i a_j (1 - k_{ij}) \quad (4)$$

$$133 \quad b = \sum_i x_i b_i \quad (5)$$

134 where  $k_{ij}$  are the binary interaction parameters, which were obtained in our previous works, with  
135 their dependence on temperature.<sup>41,42</sup> Here, only binary interaction parameters for the new  
136 binary hydrocarbon systems, namely  $\{n\text{-octane} + \text{benzene}\}$ ,  $\{n\text{-heptane} + \text{benzene}\}$  and  $\{n\text{-}$   
137  $\text{octane} + \text{toluene}\}$ , are regressed from binary VLE data.

138 It is worth mentioning that two different  $k_{ij}$  values were used for some  $\{\text{hydrocarbon} + \text{IL}\}$   
139 systems at 403.2 K, since those regressed from binary VLE data were not capable to describe  
140 ternary VLE data at 403.2 K or above.<sup>41,42</sup> In any case, the corrections made in previous  
141 works<sup>41,42</sup> for some systems at 403.2 K are maintained here to ensure the transferability in  
142 ternary systems. All  $k_{ij}$  values are collected in Table S1 in the Supporting Information.

## 143 4. Results and Discussion

### 144 4.1. VLE for {Aliphatic + Aromatic} Binary Systems: CPA EoS Description of Literature 145 Data

146 The VLE data for {*n*-octane + benzene}, {*n*-heptane + benzene} and {*n*-octane + toluene}  
147 binary systems were taken from literature.<sup>48</sup> These systems were further modeled in the  
148 temperature range of (323.2 – 403.2) K with the CPA EoS obtained in previous works.<sup>41,42</sup> The  
149 results are depicted in Figure S1 in the Supporting Information. The ability of the CPA EoS to  
150 describe these systems, using binary interaction parameters,  $k_{12}$ , with a small temperature  
151 dependency, is here shown. Binary interaction parameters are depicted in Table S1 in the  
152 Supporting Information along with the other binary interaction parameters for this work.

### 153 4.2. VLE/VLLE for {Aliphatic + Aromatic + IL} Ternary Systems: Experimental and 154 CPA EoS Description

155 The VLE/VLLE data for the {aliphatic + aromatic + IL} ternary systems were determined at  
156 323.2, 363.2 and 403.2 K in the whole hydrocarbon composition range and for an S/F of 10, as  
157 reported in Tables S2-S7 in the Supporting Information and depicted in Figures 1 - 6 ( $y$ - $x$  and  
158  $p$ - $x,y$  phase diagrams). This S/F was selected as the optimal for modelling purposes as discussed  
159 previously.<sup>39,41,42</sup> It can be noted that liquid-liquid phase splitting is found for all ternary  
160 systems, except for the {*n*-heptane + benzene + [C<sub>2</sub>C<sub>1</sub>im][TCM] or [4-C<sub>4</sub>C<sub>1</sub>py][TCM]} ternary  
161 systems at 403.2 K. In other words, it is not possible to avoid heterogenous equilibrium for the  
162 systems containing *n*-octane at the conditions studied in this work. The lower solubility of *n*-  
163 octane in the ILs compared with other linear aliphatic hydrocarbons with shorter alkyl chains  
164 makes it more difficult to achieve the homogeneity in the liquid phase.<sup>42</sup> Nevertheless, this fact  
165 does not imply that the VLE region in the whole composition range could not be found in more  
166 favorable conditions, especially taking into account that the *n*-octane mass fraction in the  
167 pyrolysis gasoline ( $w_{n\text{-octane}} = 0.116$ ) does not result in a heterogeneous equilibrium. In fact, in  
168 a previous work,<sup>36</sup> the COSMO-based/Aspen methodology was used to simulate the BTX  
169 extractive distillation from pyrolysis gasoline, finding homogenous extractive distillation along  
170 the whole column after properly validating COSMO predictions against experimental data. The  
171 [C<sub>2</sub>C<sub>1</sub>im][TCM] was used as mass agent with a S/F ratio of 5 and the feed was preheated up to  
172 its bubble point. Considering the slightly lower BTX solubilities predicted by COSMO, more  
173 favorable S/F ratios are expected in an optimized design.<sup>36</sup>

1  
2 174 Regarding the effect of temperature, two opposing trends are observed on all {aliphatic +  
3  
4 175 aromatic + IL} ternary systems studied, in accordance with those previously observed for other  
5  
6 176 similar systems. On the one hand, the higher the temperature, the larger the VLE region. On the  
7  
8 177 other hand, the separation effectiveness slightly decreases by the increase in temperature. In  
9  
10 178 addition, the equilibrium pressure for 363.2 and 403.2 K is around atmospheric pressure for all  
11  
12 179 ternary systems studied here. Therefore, the temperature profile in a hypothetical extractive  
13  
14 180 distillation column operating at atmospheric pressure would be not far from the temperatures  
15  
16 181 studied in this work, as well as the aliphatic/aromatic relative volatilities.

16 182 The most difficult separation of the overall BTX extractive distillation from pyrolysis gasoline  
17  
18 183 is the *n*-octane/benzene separation, *i.e.* light and heavy key components of the pyrolysis  
19  
20 184 gasoline model, respectively. Considering that *n*-octane/benzene relative volatility without IL  
21  
22 185 is lower than 1, the addition of the IL to this separation is quite remarkable. The highest  
23  
24 186 alkane/aromatic relative volatilities in this work are obtained for the {*n*-heptane + benzene +  
25  
26 187 IL} ternary systems, followed by the {*n*-octane + toluene + IL}, as expected since the flipping  
27  
28 188 phenomenon is not as pronounced as for the {*n*-octane + benzene + ionic liquid} system.

28 189 Additionally, to analyze the distribution of the hydrocarbons between the IL-free and IL-rich  
29  
30 190 liquid phases, LLE has been plotted in Figures 7 and 8 at 323.2 and 363.2 K. LLE data are  
31  
32 191 reported in Tables S1-S6 in the Supporting Information together with VLE data. At 403.2 K,  
33  
34 192 the LLE could not be determined due to technical limitations. Accordingly, only homogeneous  
35  
36 193 liquid, VLE region, is available to validate CPA EoS predictions in those cases.

36 194 Analyzing the ternary LLE diagrams, the typical wide immiscibility region of IL-containing  
37  
38 195 ternary systems is observed. In these cases, it is larger than in previously studied systems due  
39  
40 196 to the lower solubility of *n*-octane and toluene in the ILs, in comparison with benzene and  
41  
42 197 aliphatic hydrocarbons with shorter alkyl chains.<sup>34,41,42</sup> This region decreases as the temperature  
43  
44 198 increases owing to an increment of the amount of vapor phase and the slight variation of the  
45  
46 199 tie-lines slope. The IL solubility in the hydrocarbon mixture (raffinate) is negligible, whereas  
47  
48 200 the non-aromatic presents very low solubility in the {aromatic + IL} mixture.

48 201 The CPA EoS previously proposed for {hydrocarbon + IL} binary systems is here used to  
49  
50 202 describe the {aliphatic + aromatic + IL} ternary systems studied.<sup>41,42</sup> Considering the ternary  
51  
52 203 systems presented here and the ternary systems modeled in previous works, the most  
53  
54 204 representative aliphatic/aromatic separations within the pyrolysis gasoline model were  
55  
56 205 modeled. In Figures 1 - 6 it can be seen the excellent description of the {aliphatic + aromatic +



1  
2 206 IL} ternary systems provided by the CPA EoS. The best description of experimental results is  
3  
4 207 obtained at lower temperatures, that is, at 323.2 and 363.2 K. For the highest temperature (403.2  
5  
6 208 K), the CPA description worsens for the ternary systems. Therefore, slight corrections of the  
7  
8 209 experimental  $k_{13}$  and  $k_{23}$  at 403.2 K were necessary for an accurate description of the ternary  
9  
10 210 systems, as it was claimed previously.<sup>41,42</sup> It is remarkable that the corrections reported for the  
11  
12 211 {*n*-hexane + benzene + IL}, {*n*-heptane + toluene + IL} and {*n*-octane + *p*-xylene + IL} ternary  
13  
14 212 systems remain effective in this work. The EoS describes the boundary between homogeneous  
15  
16 213 and heterogeneous region, even at 403.2 K, and both *p*-*x,y* and *y*-*x* diagrams are well-fitted and  
17  
18 214 the ternary liquid-liquid equilibria is also accurately described.. The model covers the  
19  
20 215 description of hydrocarbons distribution and solubility boundaries, such as the negligible  
21  
22 216 solubility of the ILs in the raffinate phase. Therefore, the ability and robustness of the CPA EoS  
23  
24 217 to describe all these {aliphatic + aromatic + IL} ternary systems, studied in this and prior works,  
25  
26 218 are demonstrated. The lack of LLE equilibrium points at 403.2 K for {*n*-octane + benzene +  
27  
28 219 IL} does not adversely affect the CPA EoS modeling, independently regressed from phase  
29  
30 220 equilibria of binary systems. It is true that we can not explicitly validate LLE described by CPA  
31  
32 221 EoS, but it was done implicitly at 323.2 and 363.2 K.  
33  
34  
35  
36  
37  
38  
39  
40  
41  
42  
43  
44  
45  
46  
47  
48  
49  
50  
51  
52  
53  
54  
55  
56  
57  
58  
59  
60

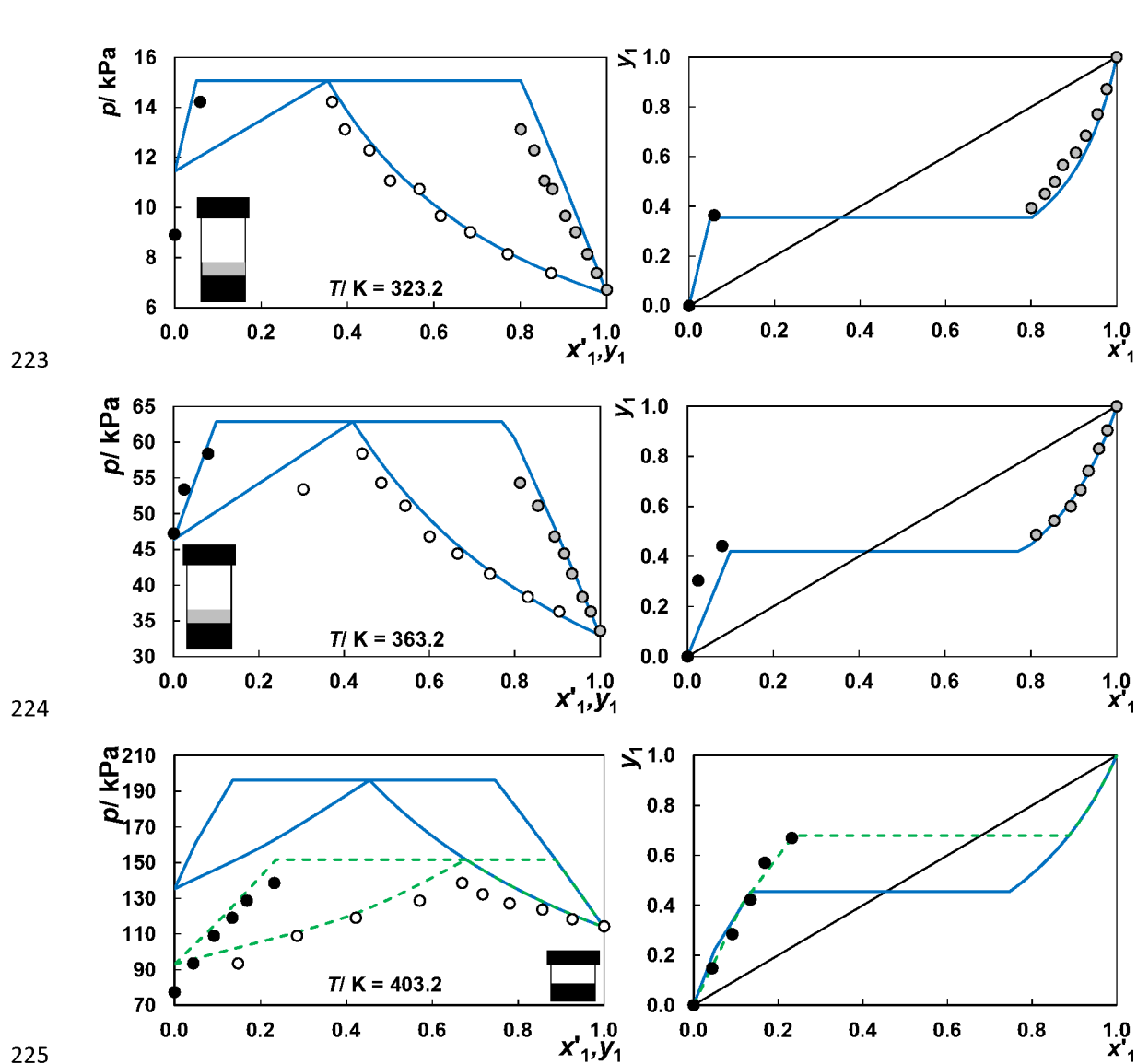
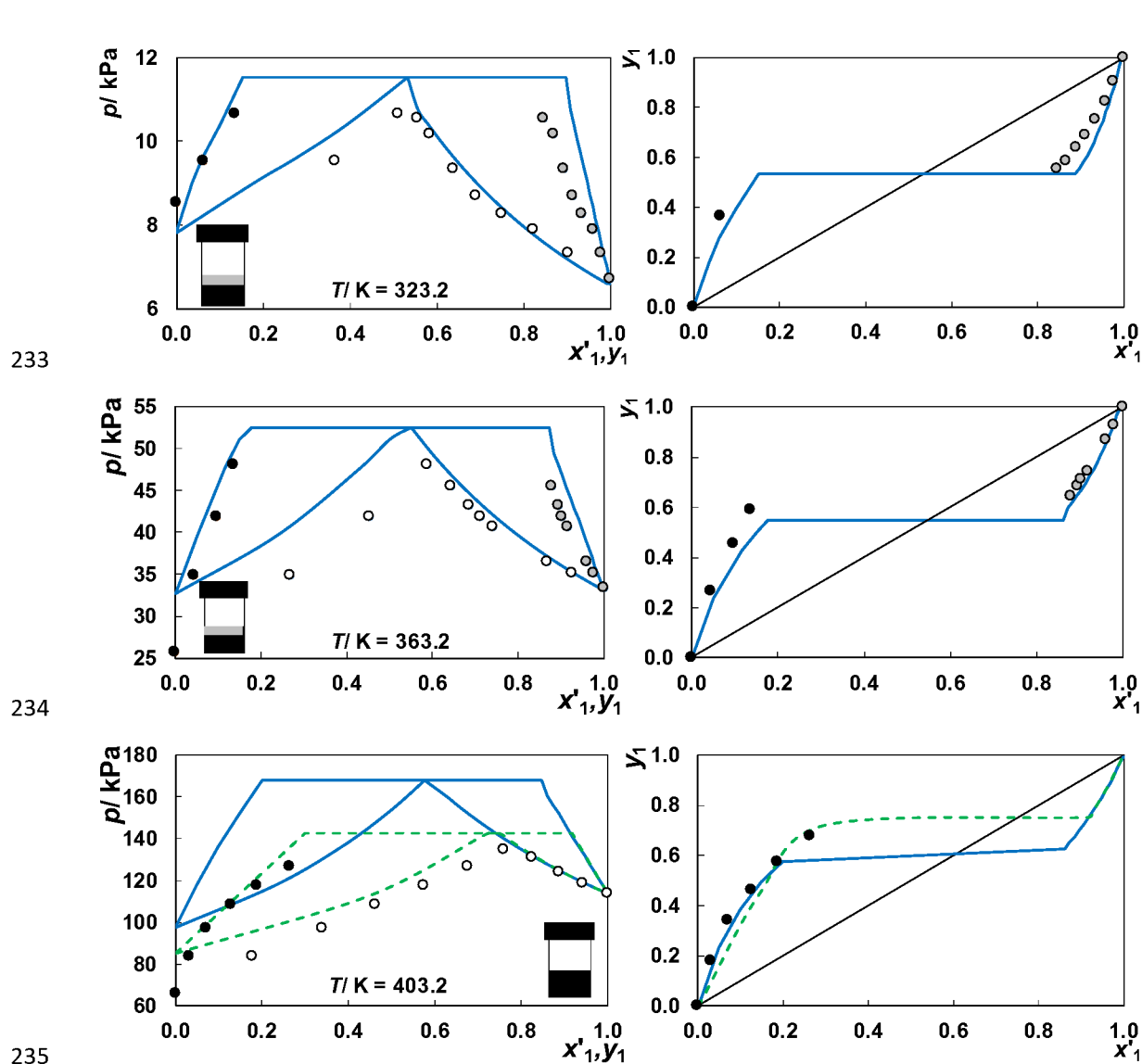


**Figure 1.**  $p$ - $xy$  and  $y$ - $x$  diagrams for the  $\{n$ -octane (1) + benzene (2) +  $[C_2C_1im][TCM]$  (3) $\}$  ternary system.  $x'_1$  refers to the IL-free  $n$ -octane liquid phase composition. Symbols: black denotes IL-rich liquid phase, grey hydrocarbon-rich liquid phase, and white vapor phase. Lines: solid represents the CPA EoS with binary interaction parameters regressed from binary VLE data and dashed indicates literature corrections for VLE ternary data at 403.2 K.<sup>41,42</sup> The schematic vial shows when VLE or VLLE is observed.



236 **Figure 2.**  $p$ - $xy$  and  $y$ - $x$  diagrams for the  $\{n$ -octane (1) + benzene (2) +  $[4$ - $C_4C_1py][TCM]$  (3) $\}$   
 237 ternary system.  $x_1'$  refers to the IL-free  $n$ -octane liquid phase composition. Symbols: black  
 238 denotes IL-rich liquid phase, grey hydrocarbon-rich liquid phase, and white vapor phase. Lines:  
 239 solid represents the CPA EoS with binary interaction parameters regressed from binary VLE  
 240 data and dashed indicates literature corrections for VLE ternary data at 403.2 K.<sup>41,42</sup> The  
 241 schematic vial shows when VLE or VLLE is observed.

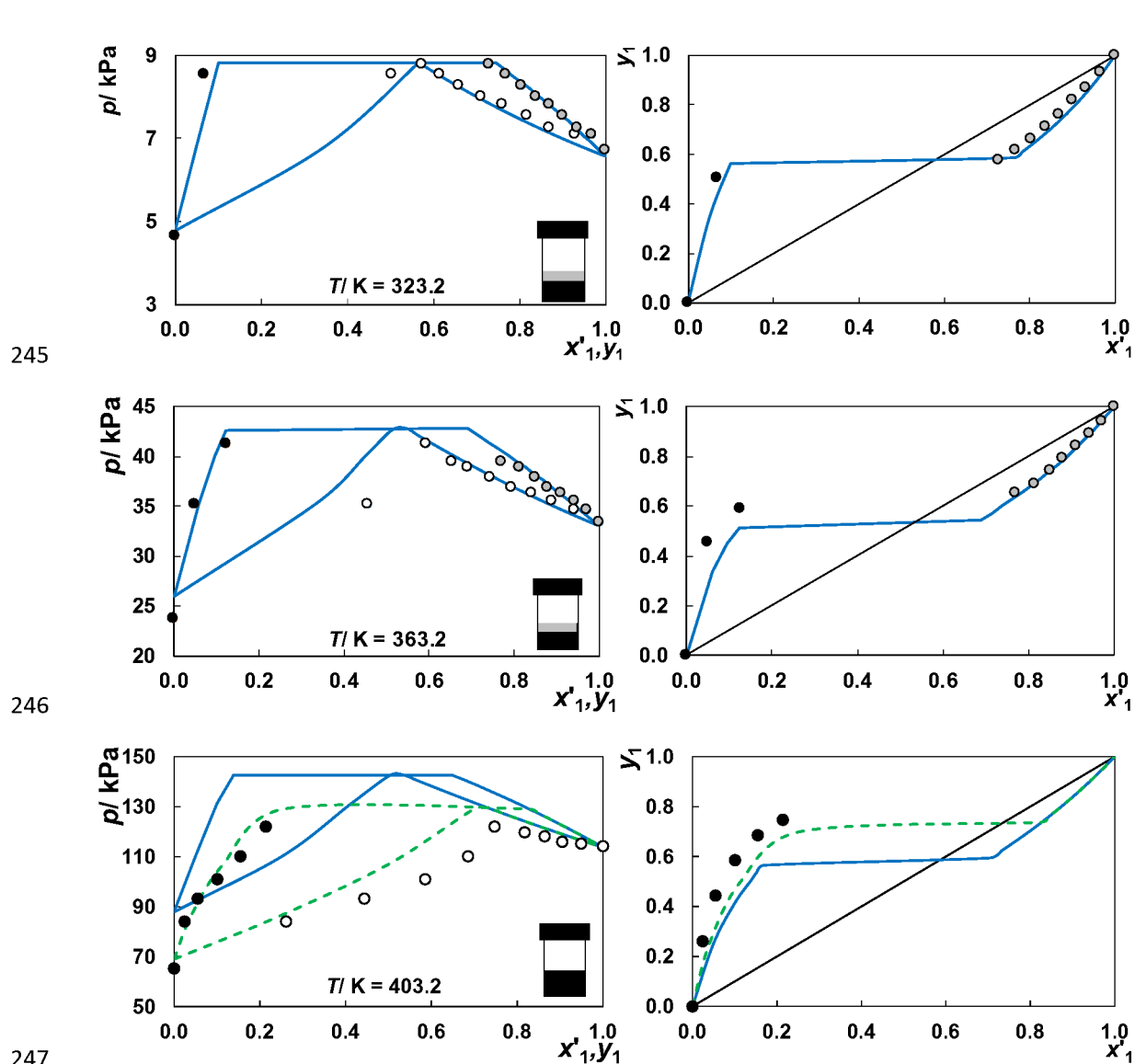


**Figure 3.**  $p$ - $x$  and  $y$ - $x$  diagrams for the  $\{n\text{-octane (1)} + \text{toluene (2)} + [\text{C}_2\text{C}_1\text{im}][\text{TCM}] (3)\}$  ternary system.  $x'_1$  refers to the IL-free  $n$ -octane liquid phase composition. Symbols: black denotes IL-rich liquid phase, grey hydrocarbon-rich liquid phase, and white vapor phase. Lines: solid represents the CPA EoS with binary interaction parameters regressed from binary VLE data and dashed indicates literature corrections for VLE ternary data at 403.2 K.<sup>41,42</sup> The schematic vial shows when VLE or VLLE is observed.

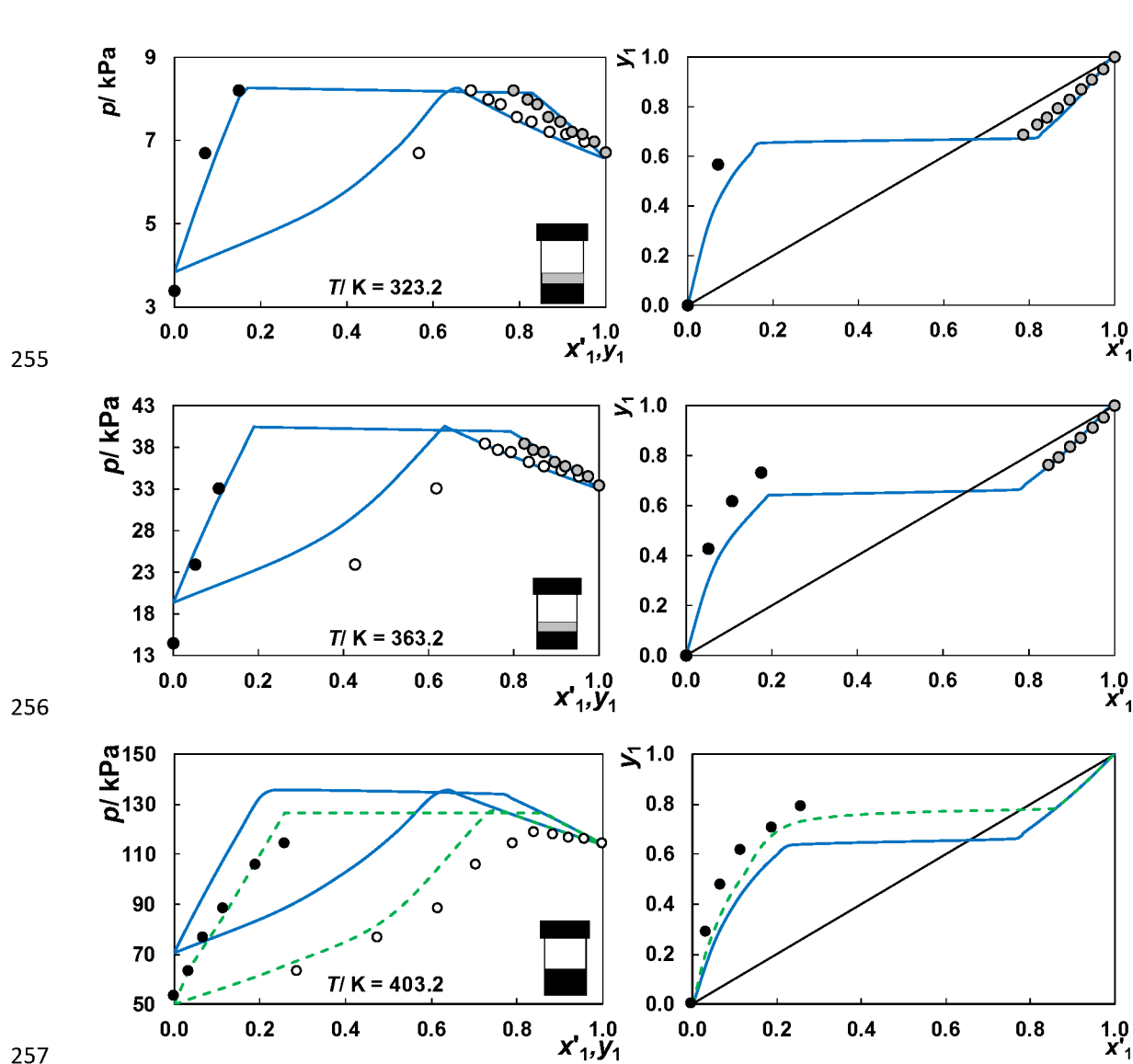


**Figure 4.**  $p$ - $x$  and  $y$ - $x$  diagrams for the  $\{n\text{-octane (1)} + \text{toluene (2)} + [4\text{-C}_4\text{C}_1\text{py}][\text{TCM}] (3)\}$  ternary system.  $x'_1$  refers to the IL-free  $n$ -octane liquid phase composition. Symbols: black denotes IL-rich liquid phase, grey hydrocarbon-rich liquid phase, and white vapor phase. Lines: solid represents the CPA EoS with binary interaction parameters regressed from binary VLE data and dashed indicates literature corrections for VLE ternary data at 403.2 K.<sup>41,42</sup> The schematic vial shows when VLE or VLLE is observed.

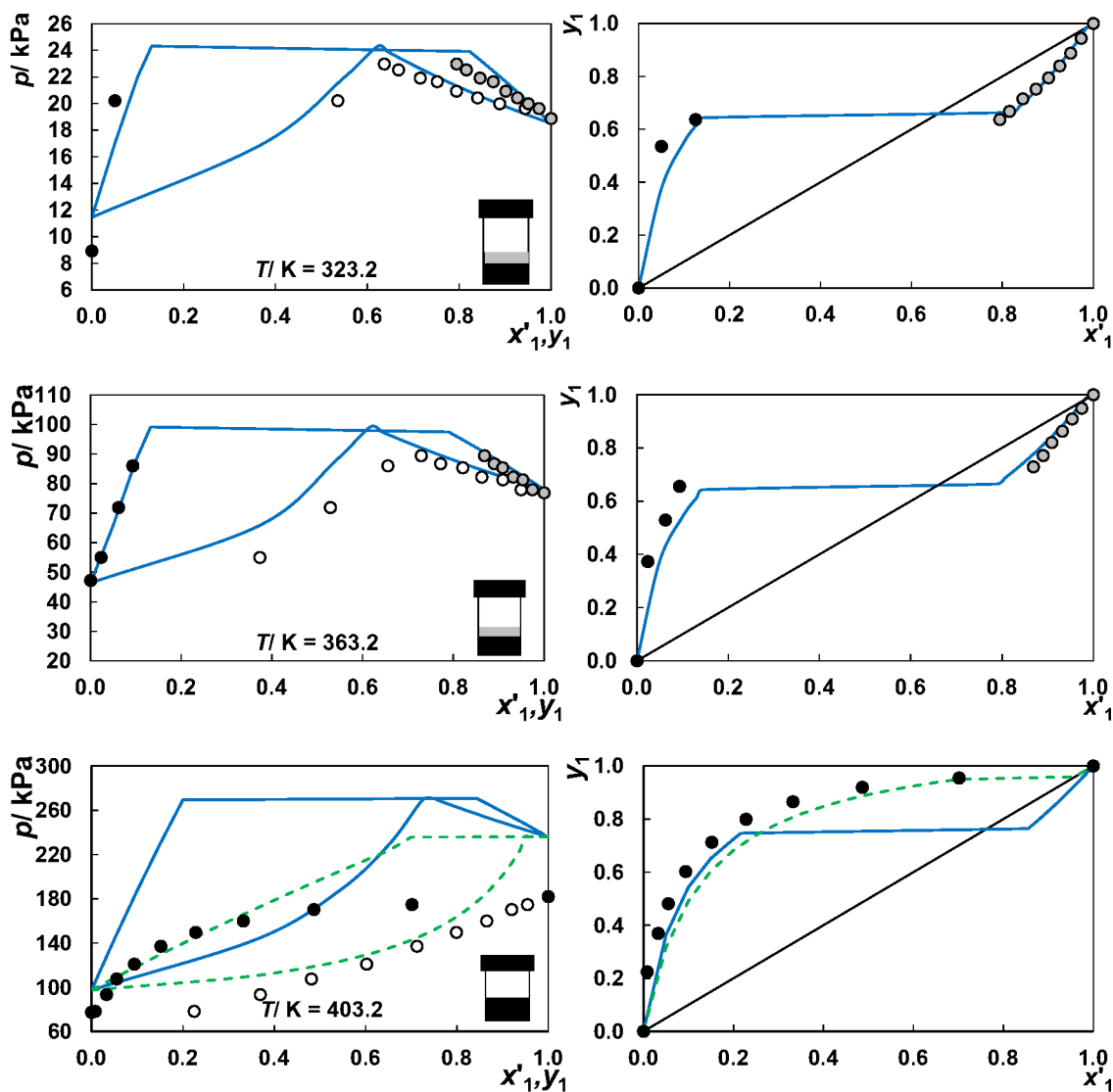


**Figure 5.**  $p$ - $x_1$  and  $y$ - $x_1$  diagrams for the  $\{n$ -heptane (1) + benzene (2) +  $[C_2C_1im][TCM]$  (3) $\}$  ternary system.  $x_1'$  refers to the IL-free  $n$ -heptane liquid phase composition. Symbols: black denotes IL-rich liquid phase, grey hydrocarbon-rich liquid phase, and white vapor phase. Lines: solid represents the CPA EoS with binary interaction parameters regressed from binary VLE data and dashed indicates literature corrections for VLE ternary data at 403.2 K.<sup>41,42</sup> The schematic vial shows when VLE or VLLE is observed.

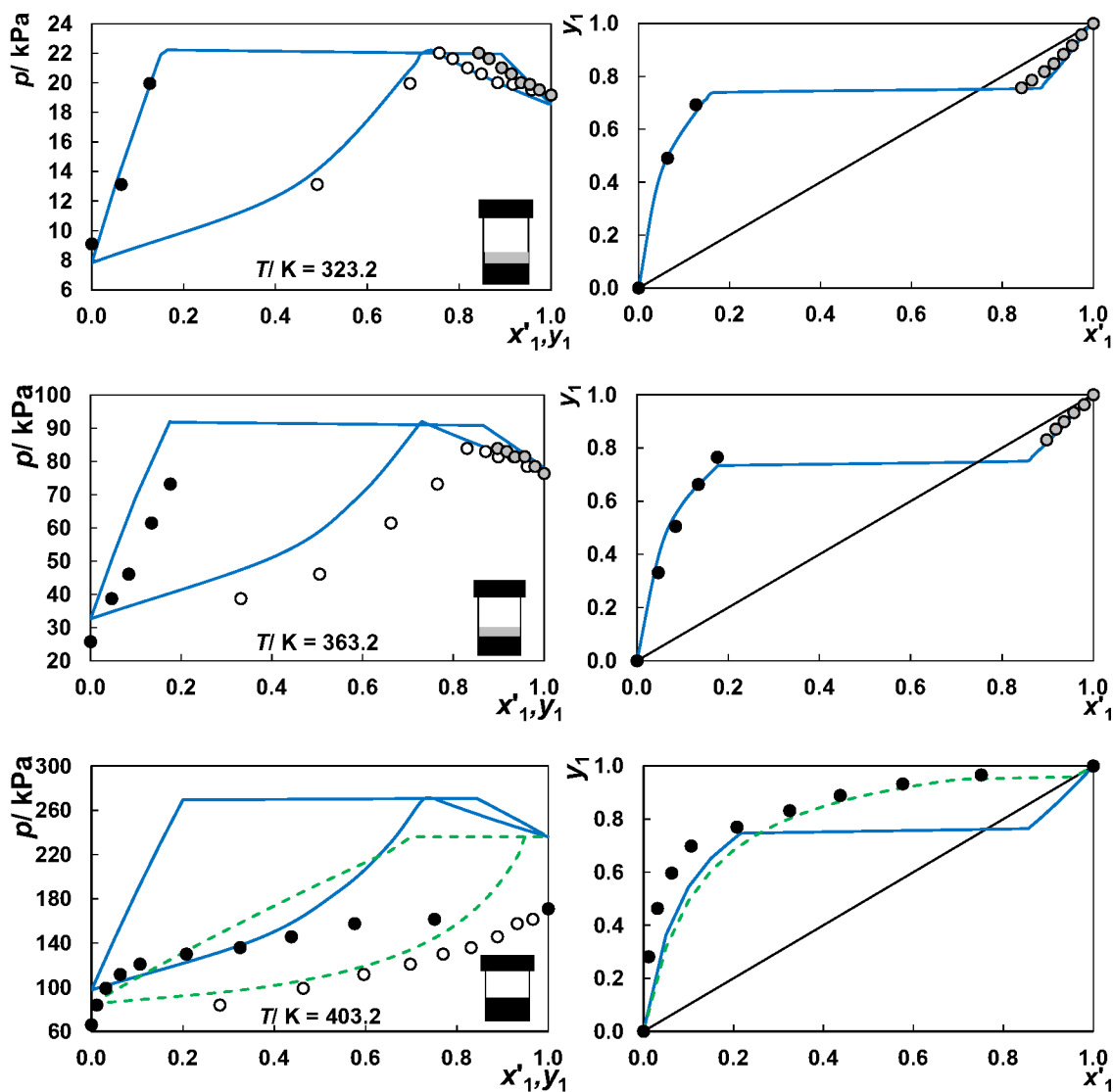


**Figure 6.**  $p$ - $xy$  and  $y$ - $x$  diagrams for the  $\{n$ -heptane (1) + benzene (2) +  $[4$ - $C_4C_1py][TCM]$  (3) $\}$  ternary system.  $x_1'$  refers to the IL-free  $n$ -heptane liquid phase composition. Symbols: black denotes IL-rich liquid phase, grey hydrocarbon-rich liquid phase, and white vapor phase. Lines: solid represents the CPA EoS with binary interaction parameters regressed from binary VLE data and dashed indicates literature corrections for VLE ternary data at 403.2 K.<sup>41,42</sup> The schematic vial shows when VLE or VLLE is observed.

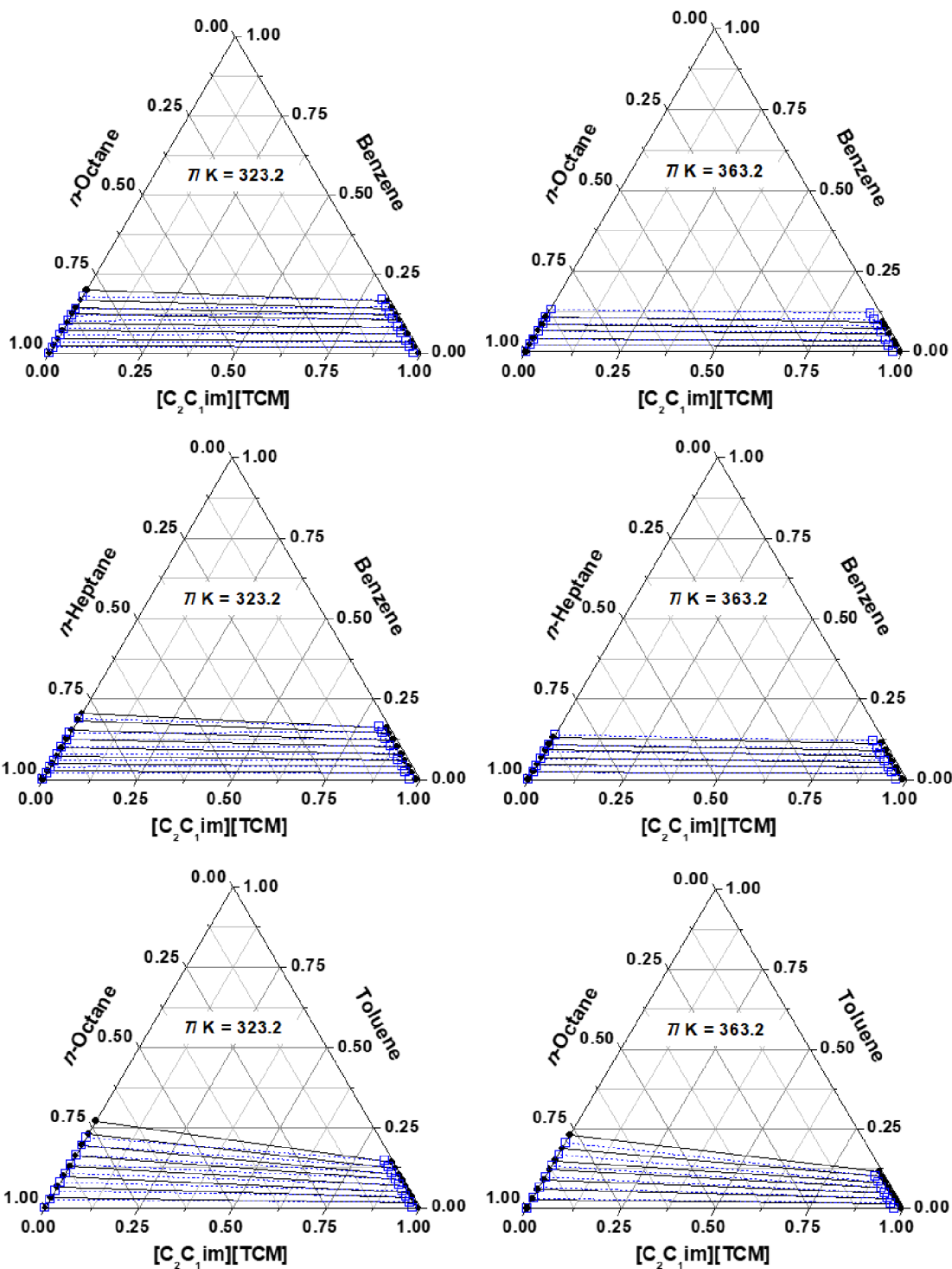


**Figure 7.** Ternary LLE diagrams from the VLLE data for the {aliphatic + aromatic + [C<sub>2</sub>C<sub>1</sub>py][TCM]} ternary system with S/F = 10. Full symbols and solid lines denote experimental data and empty squares and dashed lines the CPA EoS.



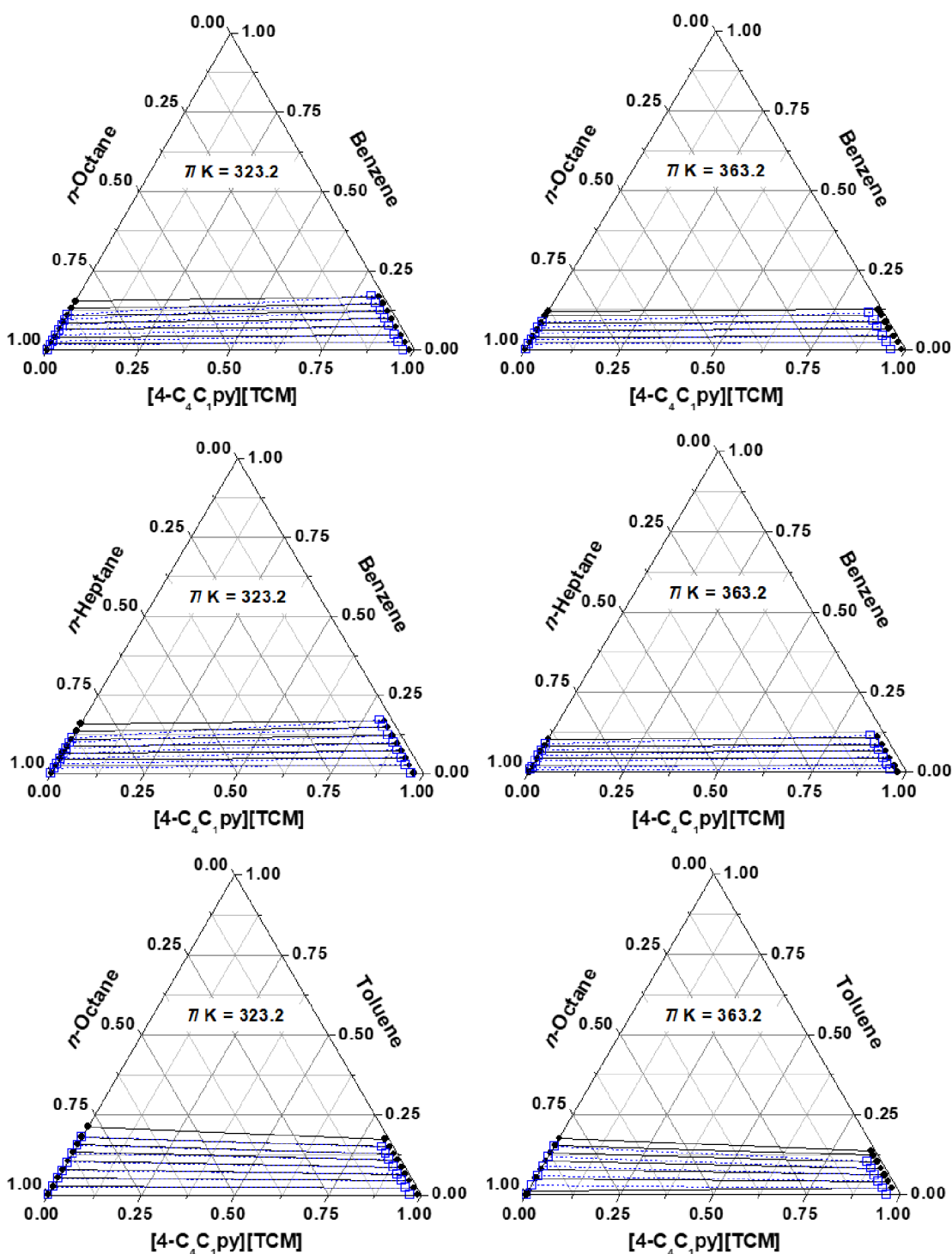


**Figure 8.** Ternary LLE diagrams from the VLLE data for the {aliphatic + aromatic + [4-C<sub>4</sub>C<sub>1</sub>py][TCM]} ternary system with S/F = 10. Full symbols and solid lines denote experimental data and empty squares and dashed lines the CPA EoS.

### 4.3. Analysis of the Aliphatic/Aromatic Relative Volatility

The aliphatic/aromatic relative volatility for each {aliphatic + aromatic + IL} ternary system has been determined from the VLE/VLLE data to quantify the effectiveness of the [TCM]-based ILs for the proposed separation. The values are reported in Tables S1-S6, in the Supporting Information, together with the VLLE data, calculated as follows:

$$\alpha_{12} = \frac{K_1}{K_2} = \frac{y_1/x_1}{y_2/x_2} \quad (10)$$

where  $y_i$  and  $x_i$  denote the molar fraction of component  $i$  in the vapor and liquid phases, respectively. The  $n$ -octane/benzene relative volatility values are depicted in Figure 9 as a function of free-IL hydrocarbon liquid molar fraction. The  $n$ -heptane/benzene and  $n$ -octane/toluene relative volatilities as a function of free-IL hydrocarbon molar fraction are reported in Figures S2 and S3 in the Supporting Information. As can be seen in Figure 9, the effectiveness of the [C<sub>2</sub>C<sub>1</sub>im][TCM] and [4-C<sub>4</sub>C<sub>1</sub>py][TCM] is quite remarkable. The  $n$ -octane/benzene relative volatility is reverse for the whole hydrocarbon composition and for all the studied temperatures, achieving values that ensure a feasible separation, values close to up 17 for 363.2 K and up to 9 for 403.2 K. The same effect is observed for the  $n$ -heptane/benzene and  $n$ -octane/toluene relative volatility.

Besides comparing the two IL performance, the best results in terms of aliphatic/aromatic relative volatility are obtained with the [4-C<sub>4</sub>C<sub>1</sub>py][TCM] for all the ternary systems, within the uncertainty, except for the { $n$ -heptane + benzene + IL} ternary system at 403.2 K. This ternary system is the only one without heterogeneity and the [C<sub>2</sub>C<sub>1</sub>im][TCM] shows higher relative volatility than the [4-C<sub>4</sub>C<sub>1</sub>py][TCM] due to its higher aromatic/aliphatic selectivity, as explained in previous works.<sup>34,39,41,42</sup> In brief, these results show the great potential of the [C<sub>2</sub>C<sub>1</sub>im][TCM] and [4-C<sub>4</sub>C<sub>1</sub>py][TCM] ILs as mass agents for the BTX extractive distillation from pyrolysis gasoline.

For the VLLE systems, the aliphatic/aromatic relative volatility remains almost constant for the homogeneous data, while decreases for the heterogeneous ones as free-IL aliphatic molar fraction increases. For the homogeneous ternary systems, *i.e.*, { $n$ -heptane + benzene + IL} at 403.2 K, the aliphatic/aromatic relative volatility decreases as the aliphatic molar fraction increases for the whole composition range. These effects are in agreement with those observed for the { $n$ -heptane + toluene + IL} ternary systems.<sup>41</sup> As expected, the [4-C<sub>4</sub>C<sub>1</sub>py][TCM] offers

the best performance when two liquid phases are present due to its higher extraction capacity, while the  $[\text{C}_2\text{C}_1\text{im}][\text{TCM}]$  stands as a better mass separating agent for homogeneous systems due to its higher selectivity for the aromatic compounds.

These behaviors are well described by the CPA EoS, confirming its great potential as a model to describe the effectiveness of both  $[\text{C}_2\text{C}_1\text{im}][\text{TCM}]$  and  $[\text{4-C}_4\text{C}_1\text{py}][\text{TCM}]$  as mass agents in the BTX extractive distillation from pyrolysis gasoline.

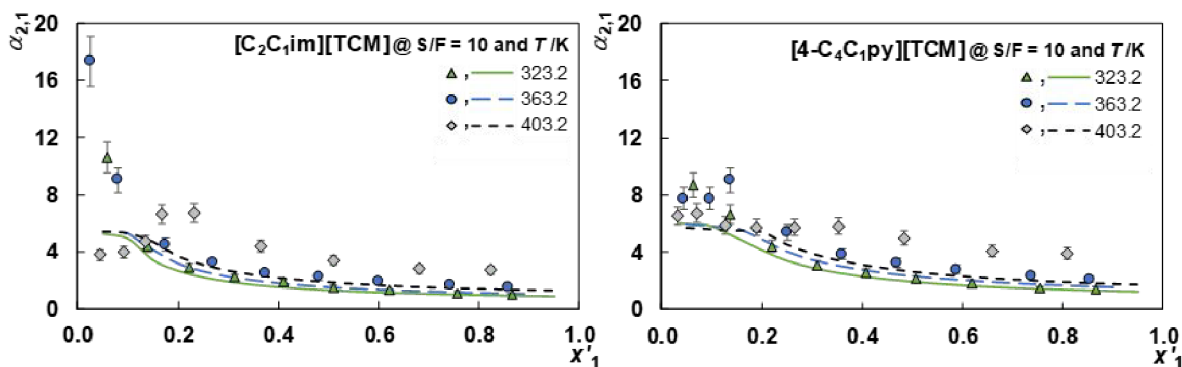


**Figure 9.** *n*-Octane/benzene relative volatility as a function of the free-IL aliphatic molar fraction for the  $\{n\text{-octane} + \text{benzene} + [\text{C}_2\text{C}_1\text{im}][\text{TCM}]/[\text{4-C}_4\text{C}_1\text{py}][\text{TCM}]\}$ . Symbols represent the experimental data and the lines the CPA EoS.

## Conclusions

In this work the VLE/VLLE for  $\{n\text{-octane} + \text{benzene} + [\text{C}_2\text{C}_1\text{im}][\text{TCM}] \text{ or } [\text{4-C}_4\text{C}_1\text{py}][\text{TCM}]\}$ ,  $\{n\text{-heptane} + \text{benzene} + [\text{C}_2\text{C}_1\text{im}][\text{TCM}] \text{ or } [\text{4-C}_4\text{C}_1\text{py}][\text{TCM}]\}$ , and  $\{n\text{-octane} + \text{toluene} + [\text{C}_2\text{C}_1\text{im}][\text{TCM}] \text{ or } [\text{4-C}_4\text{C}_1\text{py}][\text{TCM}]\}$  ternary systems were determined by HS-GC at 323.2, 363.2 and 403.2 K and for a S/F ratio of 10. The results have shown the great effectiveness of these two ILs for the three aliphatic/aromatic separations. The aliphatic/aromatic relative volatility has been reversed in the whole hydrocarbon composition range for the *n*-octane/benzene separation, *i.e.* the most challenging separation, and the closer ones. Furthermore, the high aliphatic/aromatic relative volatilities obtained suggest a highly favorable BTX recover from pyrolysis gasoline.

The VLE/VLLE data were modeled by the CPA EoS model previously obtained from the VLLE data from different  $\{\text{hydrocarbon} + [\text{C}_2\text{C}_1\text{im}][\text{TCM}] \text{ or } [\text{4-C}_4\text{C}_1\text{py}][\text{TCM}]\}$  binary systems. The description of the phase equilibria and the transition from the VLE to VLLE region was verified in this work, using the same binary interaction parameters gathered in previous systems and

1  
2 356 their small temperature dependency. Moreover, the slight corrections made to describe better  
3  
4 357 the ternary systems previously studied, remain effective for the systems here reported.  
5  
6 358 Therefore, the accuracy and robustness of the modeling proposal were demonstrated. The bases  
7  
8 359 to implement the CPA EoS model on a commercial simulator to rigorously simulate the  
9  
10 360 multicomponent BTX extractive distillation from pyrolysis gasoline with [TCM]-based ILs  
11  
12 361 have been established.

13 362

### 15 363 **Supporting Information**

17  
18 364 CPA EoS binary interaction parameters. VLE/VLLE for {*n*-octane + benzene +  
19  
20 365 [C<sub>2</sub>C<sub>1</sub>im][TCM] or [4-C<sub>4</sub>C<sub>1</sub>py][TCM]}, {*n*-heptane + benzene + [C<sub>2</sub>C<sub>1</sub>im][TCM] or [4-  
21  
22 366 C<sub>4</sub>C<sub>1</sub>py][TCM]}, and {*n*-octane + toluene + [C<sub>2</sub>C<sub>1</sub>im][TCM] or [4-C<sub>4</sub>C<sub>1</sub>py][TCM]} ternary  
23  
24 367 systems. VLE for {*n*-octane + benzene}, {*n*-heptane + benzene} and {*n*-octane + toluene}  
25  
26 368 binary systems. Aliphatic/aromatic relative volatility for *n*-heptane + benzene +  
27  
28 369 [C<sub>2</sub>C<sub>1</sub>im][TCM] or [4-C<sub>4</sub>C<sub>1</sub>py][TCM]} and {*n*-octane + toluene + [C<sub>2</sub>C<sub>1</sub>im][TCM] or [4-  
29  
30 370 C<sub>4</sub>C<sub>1</sub>py][TCM]} ternary systems.

31 371

### 33 372 **Funding Sources**

35  
36 373 This work was partly developed in the scope of the project CICECO-Aveiro Institute of  
37  
38 374 Materials, UIDB/50011/2020 & UIDP/50011/2020, financed by national funds through the  
39  
40 375 Portuguese Foundation for Science and Technology/MCTES. The authors are also grateful to  
41  
42 376 Ministerio de Economía y Competitividad (MINECO) of Spain and Comunidad Autónoma de  
43  
44 377 Madrid for financial support of Projects CTQ2017–85340-R and P2018/EMT-4348,  
45  
46 378 respectively. P.N. and P.J.C. thank FCT for awarding their postdoctoral grant  
47  
48 379 (SFRH/BPD/117084/2016) and contract under the Investigator FCT 2015 (IF/00758/2015),  
49  
50 380 respectively. N.D.-M. and M.A. also thank MINECO for awarding them an FPI grant (BES–  
51  
52 381 2015–072855 and PRE2018-083728, respectively). M.L thanks Ministerio de Educación,  
53  
54 382 Cultura y Deporte of Spain for awarding him a José Castillejo postdoctoral mobility grant  
55  
56 383 (CAS17/00018). All authors thank Infochem-KBC for the Multiflash program that was used for  
57  
58 384 the CPA EoS calculations.

385 **References**

- 386 (1) Franck, H. G.; Stadelhofer, J. W. *Industrial Aromatic Chemistry*; Springer-Verlag:  
387 Berlin, 1988.
- 388 (2) Gary, J. H.; Handwerk, G. E. *Petroleum Refining. Technology and Economics*, Fourth  
389 Edi.; Marcel Dekker: New York, 2001.
- 390 (3) Seader, J. D.; Henley, E. J.; Roper, D. K. *Separation Process Principles*, 3rd ed.; John  
391 Wiley & Sons, 2009.
- 392 (4) Meyers, Ro. A. *Handbook of Petroleum Refining Processes*; 2003.
- 393 (5) Lei, Z.; Li, C.; Chen, B. Extractive Distillation: A Review. *Sep. Purif. Rev.* **2003**, *32*  
394 (2), 121–213. <https://doi.org/10.1081/SPM-120026627>.
- 395 (6) Momoh, S. O. Assessing the Accuracy of Selectivity as a Basis for Solvent Screening  
396 in Extractive Distillation Processes. *Sep. Sci. Technol.* **1991**, *26* (5), 729–742.  
397 <https://doi.org/10.1080/01496399108049911>.
- 398 (7) Kossack, S.; Kraemer, K.; Gani, R.; Marquardt, W. A Systematic Synthesis Framework  
399 for Extractive Distillation Processes. *Chem. Eng. Res. Des.* **2008**, *86* (7), 781–792.  
400 <https://doi.org/10.1016/j.cherd.2008.01.008>.
- 401 (8) Gerbaud, V.; Rodriguez-Donis, I.; Hegely, L.; Lang, P.; Denes, F.; You, X. Q. Review  
402 of Extractive Distillation. Process Design, Operation, Optimization and Control. *Chem.*  
403 *Eng. Res. Des.* **2019**, *141*, 229–271. <https://doi.org/10.1016/j.cherd.2018.09.020>.
- 404 (9) Lek-utaiwan, P.; Suphanit, B.; Douglas, P. L.; Mongkolsiri, N. Design of Extractive  
405 Distillation for the Separation of Close-Boiling Mixtures: Solvent Selection and  
406 Column Optimization. *Comput. Chem. Eng.* **2011**, *35* (6), 1088–1100.  
407 <https://doi.org/10.1016/j.compchemeng.2010.12.005>.
- 408 (10) Medina-Herrera, N.; Grossmann, I. E.; Mannan, M. S.; Jiménez-Gutiérrez, A. An  
409 Approach for Solvent Selection in Extractive Distillation Systems Including Safety  
410 Considerations. *Ind. Eng. Chem. Res.* **2014**, *53* (30), 12023–12031.  
411 <https://doi.org/10.1021/ie501205j>.
- 412 (11) Wang, Y.; Liang, S.; Bu, G.; Liu, W.; Zhang, Z.; Zhu, Z. Effect of Solvent Flow Rates  
413 on Controllability of Extractive Distillation for Separating Binary Azeotropic Mixture.  
414 *Ind. Eng. Chem. Res.* **2015**, *54* (51), 12908–12919.  
415 <https://doi.org/10.1021/acs.iecr.5b03666>.
- 416 (12) Rogers, R. D.; Seddon, K. R. Perspective Article: Ionic Liquids Solvents of the Future?  
417 *Science (80-. )*. **2003**, *302*, 792–793. <https://doi.org/10.1126/science.1090313>.
- 418 (13) Navarro, P.; Larriba, M.; Rojo, E.; García, J.; Rodríguez, F. Thermal Properties of  
419 Cyano-Based Ionic Liquids. *J. Chem. Eng. Data* **2013**, *58* (8), 2187–2193.  
420 <https://doi.org/10.1021/jc400140n>.
- 421 (14) Canales, R. I.; Brennecke, J. F. Comparison of Ionic Liquids to Conventional Organic  
422 Solvents for Extraction of Aromatics from Aliphatics. *J. Chem. Eng. Data* **2016**, *61* (5),  
423 1685–1699. <https://doi.org/10.1021/acs.jced.6b00077>.
- 424 (15) Larriba, M.; Navarro, P.; García, J.; Rodríguez, F. Extraction of Benzene ,  
425 Ethylbenzene , and Xylenes from n -Heptane Using Binary Mixtures of [ 4empy ][ Tf 2  
426 N ] and [ Emim ][ DCA ] Ionic Liquids. *Fluid Phase Equilib.* **2014**, *380*, 1–10.  
427 <https://doi.org/10.1016/j.fluid.2014.07.034>.
- 428 (16) Larriba, M.; Navarro, P.; González, E. J.; García, J.; Rodríguez, F. Separation of BTEX  
429 from a Naphtha Feed to Ethylene Crackers Using a Binary Mixture of [4empy][Tf2N]  
430 and [Emim][DCA] Ionic Liquids. *Sep. Purif. Technol.* **2015**, *144*, 54–62.  
431 <https://doi.org/10.1016/j.seppur.2015.02.021>.
- 432 (17) Larriba, M.; de Riva, J.; Navarro, P.; Moreno, D.; Delgado-Mellado, N.; García, J.;

- 1  
2 433 Ferro, V. R.; Rodríguez, F.; Palomar, J. COSMO-Based/Aspen Plus Process  
3 434 Simulation of the Aromatic Extraction from Pyrolysis Gasoline Using the  
4 435 {[4empy][NTf<sub>2</sub>] + [Emim][DCA]} Ionic Liquid Mixture. *Sep. Purif. Technol.* **2018**,  
5 436 *190* (September 2017), 211–227. <https://doi.org/10.1016/j.seppur.2017.08.062>.
- 6 437 (18) Navarro, P.; Larriba, M.; García, J.; Rodríguez, F. Design of the Hydrocarbon  
7 438 Recovery Section from the Extract Stream of the Aromatic Separation from Reformer  
8 439 and Pyrolysis Gasolines Using a Binary Mixture of [4empy][Tf<sub>2</sub>N] + [Emim][DCA]  
9 440 Ionic Liquids. *Energy and Fuels* **2017**, *31* (1), 1035–1043.  
10 441 <https://doi.org/10.1021/acs.energyfuels.6b03068>.
- 11 442 (19) Lei, Z.; Dai, C.; Zhu, J.; Chen, B. Extractive Distillation with Ionic Liquids: A Review.  
12 443 *AIChE J.* **2014**, *60*, 3312–3329. <https://doi.org/10.1002/aic.14537>.
- 13 444 (20) Kulajanpeng, K.; Suriyapraphadilok, U.; Gani, R. Systematic Screening Methodology  
14 445 and Energy Efficient Design of Ionic Liquid-Based Separation Processes. *J. Clean.*  
15 446 *Prod.* **2016**, *111* (Part A), 93–107. <https://doi.org/10.1016/j.jclepro.2015.07.052>.
- 16 447 (21) Peng-Noo, W.; Kulajanpeng, K.; Gani, R.; Suriyapraphadilok, U. *Design of Separation*  
17 448 *Processes with Ionic Liquids*; Elsevier, 2015; Vol. 37. [https://doi.org/10.1016/B978-0-](https://doi.org/10.1016/B978-0-444-63577-8.50066-8)  
18 449 [444-63577-8.50066-8](https://doi.org/10.1016/B978-0-444-63577-8.50066-8).
- 19 450 (22) Orchillés, A. V.; Miguel, P. J.; González-Alfaro, V.; Vercher, E.; Martínez-Andreu, A.  
20 451 1-Ethyl-3-Methylimidazolium Dicyanamide as a Very Efficient Entrainer for the  
21 452 Extractive Distillation of the Acetone + Methanol System. *J. Chem. Eng. Data* **2012**,  
22 453 *57* (2), 394–399. <https://doi.org/10.1021/je200972w>.
- 23 454 (23) Dai, C.; Lei, Z.; Xi, X.; Zhu, J.; Chen, B. Extractive Distillation with a Mixture of  
24 455 Organic Solvent and Ionic Liquid as Entrainer. *Ind. Eng. Chem. Res.* **2014**, *53* (40),  
25 456 15786–15791. <https://doi.org/10.1021/ie502487n>.
- 26 457 (24) Song, Z.; Li, X.; Chao, H.; Mo, F.; Zhou, T.; Cheng, H.; Chen, L.; Qi, Z. Computer-  
27 458 Aided Ionic Liquid Design for Alkane/Cycloalkane Extractive Distillation Process.  
28 459 *Green Energy Environ.* **2019**, No. xxxx. <https://doi.org/10.1016/j.gee.2018.12.001>.
- 29 460 (25) Winnert, J. M.; Devi, V. K. P. J.; Brennecke, J. F. Using Dialkylimidazolium Ionic  
30 461 Liquids to Break the Methanol + Methyl Acetate Azeotrope. *Ind. Eng. Chem. Res.*  
31 462 **2019**, *58* (50), 22633–22639. <https://doi.org/10.1021/acs.iecr.9b05760>.
- 32 463 (26) Navarro, P.; Ovejero-pérez, A.; Ayuso, M.; Delgado-mellado, N.; Larriba, M.; García,  
33 464 J.; Rodríguez, F. Cyclohexane / Cyclohexene Separation by Extractive Distillation with  
34 465 Cyano-Based Ionic Liquids. *J. Mol. Liq.* **2019**, *289*, 111120.  
35 466 <https://doi.org/10.1016/j.molliq.2019.111120>.
- 36 467 (27) Rodríguez-Cabo, B.; Arce, A.; Soto, A. Desulfurization of Fuels by Liquid-Liquid  
37 468 Extraction with 1-Ethyl-3-Methylimidazolium Ionic Liquids. *Fluid Phase Equilib.*  
38 469 **2013**, *356*, 126–135. <https://doi.org/10.1016/j.fluid.2013.07.028>.
- 39 470 (28) Han, J.; Lei, Z.; Dong, Y.; Dai, C.; Chen, B. Process Intensification on the Separation  
40 471 of Benzene and Thiophene by Extractive Distillation. *AIChE J.* **2015**, *61* (12), 4470–  
41 472 4480. <https://doi.org/10.1002/aic.15009>.
- 42 473 (29) Jongmans, M. T. G.; Schuur, B.; De Haan, A. B. Ionic Liquid Screening for  
43 474 Ethylbenzene/Styrene Separation by Extractive Distillation. *Ind. Eng. Chem. Res.* **2011**,  
44 475 *50* (18), 10800–10810. <https://doi.org/10.1021/ie2011627>.
- 45 476 (30) Jongmans, M. T. G.; Trampé, J.; Schuur, B.; de Haan, A. B. Solute Recovery from  
46 477 Ionic Liquids: A Conceptual Design Study for Recovery of Styrene Monomer from [4-  
47 478 Mebupy][BF<sub>4</sub>]. *Chem. Eng. Process. Process Intensif.* **2013**, *70*, 148–161.  
48 479 <https://doi.org/10.1016/j.cep.2013.04.007>.
- 49 480 (31) Quijada-Maldonado, E.; Meindersma, G. W.; De Haan, A. B. Pilot Plant Study on the  
50 481 Extractive Distillation of Toluene-Methylcyclohexane Mixtures Using NMP and the  
51 482 Ionic Liquid [Hmim][TCB] as Solvents. *Sep. Purif. Technol.* **2016**, *166*, 196–204.

- 1  
2 483 <https://doi.org/10.1016/j.seppur.2016.04.041>.
- 3 484 (32) Richard, B.; Bustam, M. A.; Gonfa, G. Separation of Benzene and Cyclohexane with  
4 485 Mixed Solvent Using Extractive Distillation. *Appl. Mech. Mater.* **2014**, *625*, 578–581.  
5 486 <https://doi.org/10.4028/www.scientific.net/AMM.625.578>.
- 6 487 (33) Gonfa, G.; Bustam, M. A.; Murugesan, T.; Man, Z.; Mutalib, A. Thiocyanate Based  
7 488 Task-Specific Ionic Liquids for Separation of Benzene and Cyclohexane. *Chem. Eng.*  
8 489 *Trans.* **2013**, *32*, 1939–1944.
- 9 490 (34) Ayuso, M.; Navarro, P.; Palma, A. M.; Larriba, M.; Delgado-Mellado, N.; García, J.;  
10 491 Rodríguez, F.; Coutinho, J. A. P. Separation of Benzene from Methylcycloalkanes by  
11 492 Extractive Distillation with Cyano-Based Ionic Liquids : Experimental and CPA EoS  
12 493 Modelling. *Sep. Purif. Technol.* **2019**, *234*, 116128.  
13 494 <https://doi.org/10.1016/j.seppur.2019.116128>.
- 14 495 (35) Ayuso, M.; Cañada-Barcala, A.; Larriba, M.; Navarro, P.; Delgado-Mellado, N.;  
15 496 García, J.; Rodríguez, F. Enhanced Separation of Benzene and Cyclohexane by  
16 497 Homogeneous Extractive Distillation Using Ionic Liquids as Entrainers. *Sep. Purif.*  
17 498 *Technol.* **2020**, 116583. <https://doi.org/10.1016/j.seppur.2020.116583>.
- 18 499 (36) Navarro, P.; Dios-garcía, I. De; Larriba, M.; Delgado-mellado, N.; Ayuso, M.; Moreno,  
19 500 D.; Palomar, J.; García, J.; Rodríguez, F. Dearomatization of Pyrolysis Gasoline by  
20 501 Extractive Distillation with 1-Ethyl- 3-Methylimidazolium Tricyanomethanide. *Fuel*  
21 502 *Process. Technol.* **2019**, *195* (May), 106156.  
22 503 <https://doi.org/10.1016/j.fuproc.2019.106156>.
- 23 504 (37) Wilfred, C. D.; Kiat, C. F.; Man, Z.; Bustam, M. A.; Mutalib, M. I. M.; Phak, C. Z.  
24 505 Extraction of Dibenzothiophene from Dodecane Using Ionic Liquids. *Fuel Process.*  
25 506 *Technol.* **2012**, *93* (1), 85–89. <https://doi.org/10.1016/j.fuproc.2011.09.018>.
- 26 507 (38) Li, J.; Li, T.; Peng, C.; Liu, H. Extractive Distillation with Ionic Liquid Entrainers for  
27 508 the Separation of Acetonitrile and Water. *Ind. Eng. Chem. Res.* **2019**, *58* (14), 5602–  
28 509 5612. <https://doi.org/10.1021/acs.iecr.8b05907>.
- 29 510 (39) Navarro, P.; Larriba, M.; Delgado-Mellado, N.; Ayuso, M.; Romero, M.; García, J.;  
30 511 Rodríguez, F. Experimental Screening towards Developing Ionic Liquid-Based  
31 512 Extractive Distillation in the Dearomatization of Refinery Streams. *Sep. Purif. Technol.*  
32 513 **2018**, *201*, 268–275. <https://doi.org/10.1021/acs.iecr.8b03804>.
- 33 514 (40) Larriba, M.; Navarro, P.; Delgado-Mellado, N.; Stanisci, V.; García, J.; Rodríguez, F.  
34 515 Separation of Aromatics from N-Alkanes Using Tricyanomethanide-Based Ionic  
35 516 Liquids: Liquid-Liquid Extraction, Vapor-Liquid Separation, and Thermophysical  
36 517 Characterization. *J. Mol. Liq.* **2016**, *223*, 880–889.  
37 518 <https://doi.org/10.1016/j.molliq.2016.09.017>.
- 38 519 (41) Navarro, P.; Ayuso, M.; Palma, A. M.; Larriba, M.; Delgado-Mellado, N.; García, J.;  
39 520 Rodríguez, F.; Coutinho, J. A. P.; Carvalho, P. J. Toluene/ n -Heptane Separation by  
40 521 Extractive Distillation with Tricyanomethanide-Based Ionic Liquids: Experimental and  
41 522 CPA EoS Modeling. *Ind. Eng. Chem. Res.* **2018**, *57* (42), 14242–14253.  
42 523 <https://doi.org/10.1021/acs.iecr.8b03804>.
- 43 524 (42) Ayuso, M.; Navarro, P.; Palma, A. M.; Larriba, M.; Delgado-Mellado, N.; García, J.;  
44 525 Rodríguez, F.; Coutinho, A. P.; Carvalho, P. J. Toward Modeling the Aromatic /  
45 526 Aliphatic Separation by Extractive Distillation with Tricyanomethanide-Based Ionic  
46 527 Liquids Using CPA EoS. **2019**, *58* (42), 19681–19692.  
47 528 <https://doi.org/10.1021/acs.iecr.9b04440>.
- 48 529 (43) Navarro, P.; Larriba, M.; García, J.; González, E. J.; Rodríguez, F. Selective Recovery  
49 530 of Aliphatics from Aromatics in the Presence of the {[4empy][Tf 2 N]} +  
50 531 [Emim][DCA]} Ionic Liquid Mixture. *J. Chem. Thermodyn.* **2016**, *96*, 134–142.  
51 532 <https://doi.org/10.1016/j.jct.2015.12.033>.

1

2

3

4

5

6

7

8

9

10

11

12

13

14

15

16

17

18

19

20

21

22

23

24

25

26

27

28

29

30

31

32

33

34

35

36

37

38

39

40

41

42

43

44

45

46

47

48

49

50

51

52

53

54

55

56

57

58

59

60

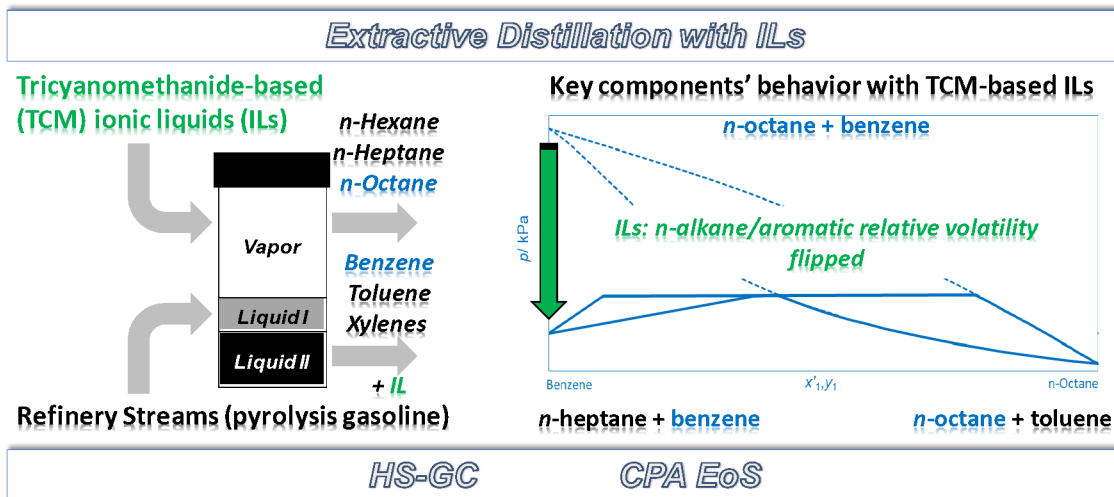
- (44) Navarro, P.; Larriba, M.; García, J.; González, E. J.; Rodríguez, F. Vapor-Liquid Equilibria of {n-Heptane+toluene+[Emim][DCA]} System by Headspace Gas Chromatography. *Fluid Phase Equilib.* **2015**, *387*, 209–216. <https://doi.org/10.1016/j.fluid.2014.12.025>.
- (45) Perry, R. H.; Green, D. W.; Maloney, J. O. *Perry's Chemical Engineers' Handbook*, 7th.; New York, 1997. <https://doi.org/10.1021/ed027p533.1>.
- (46) Kontogeorgis, G. M.; Michelsen, M. L.; Folas, G. K.; Derawi, S.; Von Solms, N.; Stenby, E. H. Ten Years with the CPA (Cubic-Plus-Association) Equation of State. Part 1. Pure Compounds and Self-Associating Systems. *Ind. Eng. Chem. Res.* **2006**, *45* (14), 4855–4868. <https://doi.org/10.1021/ie051305v>.
- (47) Kontogeorgis, G. M.; Michelsen, M. L.; Folas, G. K.; Derawi, S.; Von Solms, N.; Stenby, E. H. Ten Years with the CPA (Cubic-Plus-Association) Equation of State. Part 2. Cross-Associating and Multicomponent Systems. *Ind. Eng. Chem. Res.* **2006**, *45* (14), 4869–4878. <https://doi.org/10.1021/ie051306n>.
- (48) Technology, A. Aspen Plus Version 9, Database. 2016.

533  
534  
535  
536  
537  
538  
539  
540  
541  
542  
543  
544  
545  
546  
547  
548  
549  
550  
551  
552  
553  
554  
555  
556  
557  
558  
559  
560  
561  
562  
563  
564  
565  
566  
567  
568  
569  
570  
571  
572  
573  
574  
575  
576  
577  
578  
579  
580  
581  
582  
583  
584  
585  
586  
587  
588  
589



Table of Contents

590  
591



592